

Temperature dependence of hole spin coherence in (In,Ga)As quantum dots measured by mode-locking and echo techniques

S. Varwig¹, A. René¹, A. Greulich¹, D. R. Yakovlev^{1,2}, D. Reuter³, A. D. Wieck³ and M. Bayer¹

¹ *Experimentelle Physik 2, Technische Universität Dortmund, 44221 Dortmund, Germany*

² *Ioffe Physical-Technical Institute, Russian Academy of Sciences, 194021 St. Petersburg, Russia and*

³ *Angewandte Festkörperphysik, Ruhr-Universität Bochum, 44780 Bochum, Germany*

The temperature dependence of the coherence time of hole spins confined in self-assembled (In,Ga)As/GaAs quantum dots is studied by spin mode-locking and spin echo techniques. Coherence times limited to about a μs are measured for temperatures below 8 K. For higher temperatures a fast drop occurs down to a few ns over a 10 K range. The hole-nuclear hyperfine interaction appears too weak to account for these limitations. We suggest that spin-orbit related interactions are the decisive sources for hole spin decoherence.

PACS numbers: 71.70.Ej, 76.60.Lz, 78.47.jm, 78.67.Hc

During recent years the spins of holes confined in III-V semiconductor quantum dots (QDs) have attracted considerable interest. This interest is related to the hole spin's hyperfine coupling to nuclear spins, which has been found to be non-negligible, in contrast to original suggestions based on the vanishing contact interaction, but still considerably reduced by an order of magnitude as compared to electron spins.^{1–3} For the electrons the hyperfine interaction has been identified as the source of spin decoherence at cryogenic temperatures;^{4,5} the transverse spin relaxation time is on the order of microseconds at these conditions,^{6,7} well below the longitudinal spin relaxation times of up to milliseconds in magnetic fields large enough for sizable two-level splittings that might be of use in quantum information.

From their reduced hyperfine coupling longer coherence times may be expected for the hole spins.⁸ However, recent studies have demonstrated that the hole spin coherence time T_2 is *not* elongated, but rather comparable to that of the electron with values on the order of a μs .^{3,9,10} The origin of this behavior is not yet understood: spin-orbit interaction as another potential spin relaxation mechanism involving phonons may be more important for holes than for electrons, but at liquid helium temperatures it should be suppressed in quantum dots with a discrete energy level structure. To obtain more insight into the problem, it might be helpful to study the temperature dependence of the hole spin coherence time.

This is the problem that we address here by exploiting the recently demonstrated hole spin mode-locking (SML) in consequence of periodic pulsed excitation of the ground state transition by circularly polarized laser light.³ By monitoring the SML signal amplitude in dependence of the laser pulse separation at various temperatures we find that the hole spin coherence time remains constant in the μs range only up to about 8 K, but then drops quickly down to nanoseconds at 20 K, approaching the lifetime of optically excited electron-hole pairs. This result is confirmed by detecting the temperature dependence of optically induced hole spin echoes. From this we conclude that spin-orbit interactions play the decisive role,

even though details of the mechanism need further elaboration.

The sample under study was grown by molecular-beam epitaxy on a (001) GaAs substrate and contains ten layers of (In,Ga)As dots, separated by 100 nm GaAs barriers. The QD density per layer is about 10^{10} cm^{-2} . The dots are nominally undoped, but it has been found in earlier studies that about half of them are singly positively charged due to residual carbon impurities.³ The sample was annealed for 30 s at a temperature of 960 °C, leading to a band gap increase such that resonant excitation by a Ti:Sapphire laser is possible. The photoluminescence (PL) spectrum in Fig. 1(a) shows the ground state emission with a maximum at 1.38 eV and a full width at half maximum (FWHM) of about 20 meV.

To study the QD spin dynamics we use a degenerate pump-probe setup with the laser energies tuned to the PL maximum. The optical axis (z -axis) is chosen parallel to the sample growth direction. Spin polarization of the QD hole is generated by a periodic train of circularly polarized pump pulses exciting the transition from the resident hole to the positively charged exciton. The spin polarization along the z -axis is monitored by measuring the ellipticity of an originally linearly polarized probe beam after transmission through the sample, which is mounted in a cryostat allowing variable temperatures T down to 2 K and magnetic fields B up to 7 T. Application of such an external magnetic field along the x -axis (Voigt geometry) leads to precessions of the hole spins about this axis.

Pump and probe pulses are taken from a Ti:Sapphire laser operating at a repetition frequency of 75.75 MHz, corresponding to a pulse separation of $T_R = 13.2 \text{ ns}$ that can be extended by a pulse picker. The pulses with a duration of 1.5 ps have a spectral width of 1 meV so that an ensemble of about 10^5 QDs is addressed. The pump pulse intensity is adjusted to a pulse area of π and the probe pulse intensity is taken five times weaker. By varying the delay between pump and probe pulses, the temporal evolution of the spin polarization is measured, as shown in Fig. 1(b).

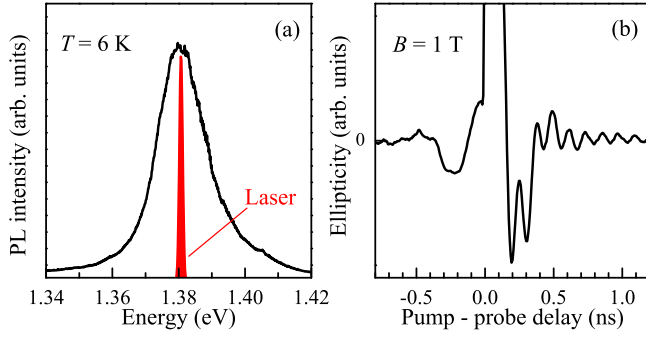


FIG. 1. (Color online) (a) Photoluminescence spectrum of the (In,Ga)As/GaAs QD ensemble, measured at $T = 6$ K. The red-colored line shows the laser spectrum with a FWHM of 1 meV which is in resonance with the QD ground state emission. (b) Pump-probe ellipticity measurement at $B = 1$ T and $T = 6$ K. The zero delay peak influenced by scattered laser light is cut off for better visibility of the spin precession oscillations.

After pump incidence at zero delay one sees damped oscillations with contributions from resident and photo-created electron and hole spins. These contributions are distinguishable by their precession frequencies due to different g -factors, namely $|g_e| = 0.58$ for electrons and $|g_h| = 0.14$ for holes. The damping of the signal arises from spin dephasing due to g -factor variations in the ensemble. In Ref. 11 we have shown that for the in-plane hole g -factor these variations are comparable in magnitude to the absolute g -factor value. Therefore the hole spin dephasing time $T_{2,h}^* \sim 0.25$ ns is quite fast, compared with the electron spin dephasing time of $T_{2,e}^* \sim 1.03$ ns.

At negative delays, before pump pulse arrival, a rephasing of the resident hole spins due to the spin mode-locking (SML) effect is visible. This rephasing arises from spins whose precession about the magnetic field becomes synchronized with the laser pulse repetition rate, as expressed by the phase synchronization condition (PSC):⁷

$$\omega = \frac{|g_h|\mu_B B}{\hbar} = N \frac{2\pi}{T_R}, \quad (1)$$

where ω is the Larmor precession frequency determined by the hole g -factor g_h along the magnetic field B , μ_B is the Bohr magneton, and N is a positive integer. Note, however, that the hole spin mode-locking amplitude is weaker by a factor of three compared to the amplitude at positive delays as a result of the rather weak hyperfine interaction: the coupling to the nuclei, if efficient, would drive modes which do not initially fulfill the PSC into spin mode-locking. This nuclear frequency focusing would occur by building up a nuclear field of proper strength that adds to the external magnetic field. While being efficient for electrons, for which after sufficiently long pumping all optically excited ones can contribute to mode-locking,¹² the hyperfine interaction for holes is too weak to induce such nuclear frequency focusing.³ As a consequence the negative delay signal is considerably

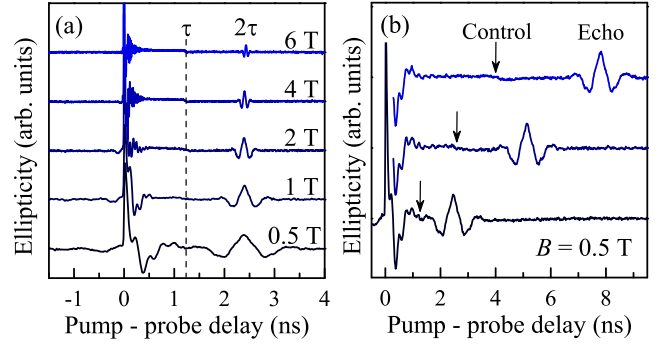


FIG. 2. (Color online) (a) Hole spin echoes at different magnetic fields, $\tau = 1.2$ ns, $T = 6$ K. Curves are shifted vertically for clarity. (b) Hole spin echoes for different control pulse delays $\tau = 1.2, 2.6$ and 3.9 ns. The echo appearance time 2τ shifts in accordance with the control pulse arrival time τ . $B = 0.5$ T and $T = 6$ K.

weaker than the one at positive delays, where the signal strength is determined by the entirety of excited dots.

For spin echo experiments an additional pulse, termed the control pulse, is introduced into the excitation scheme. This pulse is taken from a second Ti:Sapphire laser system synchronized with the first one with a 100 fs accuracy, but independently tunable in photon energy. Pulse duration and spectral width are equal for the two lasers. The second laser is used to rotate the hole spins about the optical z -axis, in analogy to experiments on electron spin rotations in (In,Ga)As/GaAs QDs.¹³ The control pulse intensity is adjusted to a pulse area of 2π in order not to populate trion states, but remain in the spin subspace of resident holes.

By adjusting the control photon energy to the pump photon energy each control pulse rotates the resident hole spins in those QDs excited by the pump pulse by an angle of π . Figure 2(a) shows spin rotation measurements at different magnetic fields varied from 0.5 to 6 T. The control pulse hits the sample at a time delay $\tau = 1.2$ ns relative to the pump pulse arrival and at a time $2\tau = 2.4$ ns a hole spin echo appears. It arises from the 180° rotation of the hole spin ensemble at delay τ by which the dephasing occurring between pump and control is inverted and the spins reconvene. The temporal sequence is confirmed when the control pulse delay τ is varied, as seen in Fig. 2(b). The time between echo formation and pump arrival is twice the time between control and pump.

The two effects, spin mode-locking and spin echo, are exploited to determine the temperature dependence of the hole spin coherence time. First we turn to the spin mode-locking signal in pure pump-probe studies without control pulses. Corresponding ellipticity traces are shown in Fig. 3(a) with focus on the mode-locking signal at negative delay times, recorded for different temperatures. The pump pulse separation was 13.2 ns. Two contributions with different frequencies are seen in the signal; the one with lower frequency is related to the hole spin pre-

cession of interest here. Because of the strong damping, even at the lowest temperatures only one full oscillation is seen. The higher frequency contribution can be assigned to the electron spin.

Clear hole spin mode-locking (SML) can be seen in Fig. 3(a) up to temperatures of 15 K. From these observations one identifies two temperature ranges, for which we have to employ different methods for extracting the hole spin coherence time T_2 . At the lower end of the studied temperatures ($T \lesssim 10$ K) T_2 is longer than the pulse repetition period T_R of 13.2 ns, such that SML can occur. The appropriate method then is to increase T_R until SML becomes weaker. From the variation of the SML amplitude with T_R , the spin coherence time can be extracted.^{3,7} Additionally, if T_2 is shorter than T_R , as apparently is the case for elevated temperatures, we can estimate the spin coherence time from the temperature dependence of the SML amplitude and the spin-echo amplitude (see below).

Let us first concentrate on the low-temperature regime. To vary T_R we implemented a pulse picker in the setup, which reduces the pulse repetition rate by letting only particular pulses of the original train pass while dumping the others. In that way we increased the time between two subsequent pump pulses incrementally from $T_R = 132$ up to 660 ns and extracted the spin mode-locking amplitude A_{SML} using a cosine fit with a Gaussian damping function. One can then determine the dependence of this amplitude on T_R and obtain the coherence time T_2 using the following relation:

$$A_{\text{SML}}(T_R) \propto \exp \left[- \left(2 + \frac{1}{2\sqrt{3} + 3} \right) \frac{T_R}{T_2} \right], \quad (2)$$

which can be found in the SOM of Ref. 7. The results for T_2 are shown in Fig. 4 by filled circles. The hole spin coherence time is constant at slightly more than 1 μ s up to almost 6-7 K, but then drops to about 100 ns at 10 K. A further temperature increase makes the SML disappear already for a pulse separation of 132 ns, which was the shortest that could technically be achieved with the pulse picker.

In the elevated temperature range $T > 10$ K the other methods need to be applied, directly exploiting the temperature dependencies of spectroscopic quantities such as the SML amplitude. While this procedure is straightforward, only estimates for T_2 can be obtained in this way. Using again a Gaussian damped cosine fit, the amplitudes of the mode-locked resident hole spin polarization in Fig. 3(a) can be extracted. These amplitudes are plotted in Fig. 3(c). The drop of the amplitude between 2 K and 15 K occurs because the spin coherence time has become comparable or shorter than the pulse separation of 13.2 ns. From the SML amplitudes before and after the drop, as seen in Fig. 3(c), one can estimate that the hole spin coherence time has to be around 7 ns at 15 K. The corresponding data point is inscribed in Fig. 4 by the vertically halved circle.

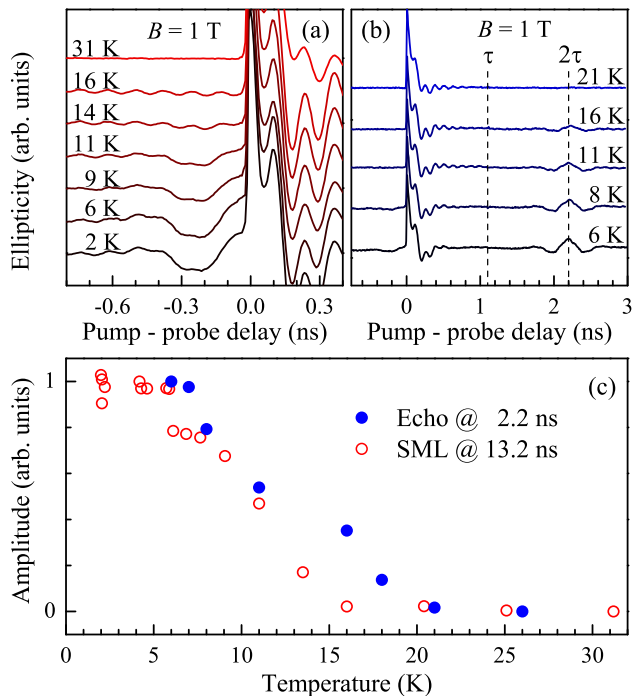


FIG. 3. (Color online) (a) Time-resolved ellipticity measurements with focus on negative delay times for different temperatures, $B = 1$ T and $T_R = 13.2$ ns. Fits to the hole spin oscillations (see text) provide the SML amplitudes (red open circles) in panel (c). (b) Hole spin echoes recorded at different temperatures for $B = 1$ T, $T_R = 13.2$ ns and $\tau = 1.1$ ns. From the echo oscillations we deduce the blue data points (solid circles) in panel (c). (c) Temperature dependence of the normalized hole spin echo (blue solid circles) and SML (red open circles) amplitudes.

Another data point can be obtained from the temperature dependence of the hole spin echo signal. In these studies the control pulse hits the dephased hole spin ensemble at 1.1 ns delay, leading to an echo at 2.2 ns, as seen in Fig. 3(b). Similar to the SML signal, the echo amplitude is constant at low temperatures, but starts to decrease strongly at around 10 K and vanishes around 20 K. For analysis, the signal around the echo is also fitted by a cosine function with a Gaussian amplitude envelope. This amplitude is plotted in Fig. 3(c), closely resembling the corresponding dependence for the SML signal. From this dependence we get a data point of $T_2 = 1$ ns at $T = 20$ K.

Figure 4 shows the temperature dependence of the hole spin coherence time and, for comparison, the electron spin coherence time in a similar quantum dot sample, published in Ref. 14. Electron and hole spin coherence times are constant at low temperatures, but then quickly decrease into the ns-range at moderate temperatures. While for the holes this decrease is very abrupt and starts at 8 K, for the electrons T_2 is constant in the μ s-range up to slightly more than 15 K before the drop occurs over a 30 K range. For the electrons the drop was associated to

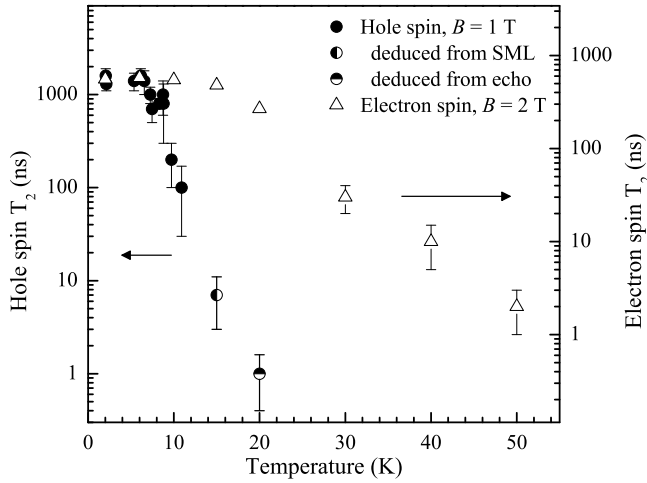


FIG. 4. Temperature dependence of the coherence time T_2 for hole spins (circles, left scale) and electron spins (triangles, right scale). The filled circles are measured by mode-locking experiments with various pulse separations at different temperatures (see text); $B = 1$ T. The vertically halved circle is deduced from the temperature dependence of the mode-locked spin amplitude with $T_R = 13.2$ ns, see Figs. 3(a) and 3(c). The horizontally halved circle is deduced from the temperature dependence of the hole spin echo, see Figs. 3(b) and 3(c). The electron data is taken from Ref. 14 being measured at $B = 2$ T. They are valid for comparison as from 1 T up to 3 T no magnetic field dependence was observed.

elastic scattering due to phonon-mediated fluctuations of the hyperfine interaction.¹⁴

Both the limitation of the hole spin coherence below a temperature of 8 K and the drop for higher temperatures need to be explained. Carrier spin coherence in quantum dots has been considered in a few works in which either hyperfine interactions or spin-orbit related interactions were addressed as sources for decoherence. Let us first discuss the works involving the nuclear bath: in the original work by Fischer and Loss¹⁵ it was shown that while the contact interaction is not relevant for holes, other contributions, the dipole-dipole interaction and the orbital angular momentum interaction with nuclear spins, can become important and may be even of comparable strength as the electron contact hyperfine interaction. Indications to that end were reported in Refs. 16.

It was recently shown, however, that the hyperfine interaction is at least an order of magnitude weaker for the holes than it is for electrons in self-assembled (In,Ga)As QDs.^{1-3,9,10,17,18} Based on these results it is unlikely that the interaction with the nuclei leads to the μ s-limit for the hole spin coherence. As mentioned, for the temperature dependence of the electron spin coherence a model was also developed based on the spectral diffusion of the nuclear-spin distribution due to excitation of acoustic phonons.^{14,19} While it works well for electrons, due to the reduced interaction strength this mechanism also seems unlikely to explain the temperature dependence for holes.

If we neglect the hole spin interaction with the nuclei, the spin-orbit interaction must account for the observed behavior of the hole spin coherence time T_2 . The hole might be excited to an excited orbital state having a different g -factor without spin-flip, resulting in a different precession frequency. After relaxation, this would lead to a phase change of the spin precession.¹⁹ In addition, the impact of anharmonic phonons due to lattice impurities, defects, etc. has been emphasized. Interactions with them can lead to a phase change in the coherent spin dynamics.¹⁹ Both mechanisms formulated for electrons are obviously also relevant for holes, potentially even more prominently as the spin-orbit interaction is stronger in the valence band.

From the splitting of about 20 meV between the first excited state and the ground state, obtained from high excitation photoluminescence studies, we estimate a splitting of the corresponding valence band states of at least 5 meV,²⁰ whereas the temperature of 8 K at which the sharp drop of T_2 sets in is considerably less than 1 meV. The excitation to excited hole states can therefore be ruled out under these conditions. Crystal defects in self-assembled QDs have been shown to be strongly suppressed, while the alloying (corresponding to some extent to implementation of impurities disturbing the crystal periodicity) broadens the phonon spectrum. In any case phonon activated mechanisms require thermal excitation to higher states, so most likely neither can be responsible for the low temperature limitation.

Consequently, we suggest here a different mechanism. For quantum dots, the interaction of carriers with acoustic phonons has been shown to have important consequences as it limits the quantum mechanical coherence of confined carriers. For example, due to it, the coherent exciton polarization drops over a timescale of a few picoseconds after pulsed carrier excitation.²¹ In the spectral domain, this scattering results in broad spectral flanks of the zero-phonon spectral line of the QD exciton transition.^{22,23} The underlying mechanism can be understood as follows: the carriers lead to the formation of a quasi-stable polaron, a bound state of the injected charges and an associated phonon population, by which the lattice becomes distorted. As a result of this distortion, a coherent phonon wave packet is emitted from the QDs, escaping on timescales of ps into the embedding material.

Another example for the importance of these phonon sidebands is the light emission from QDs into a laser resonator mode, as not only the dots in resonance with this mode contribute to the emission, but also off-resonant quantum dots in which the carriers can recombine and the photon is funneled into the laser mode with simultaneous phonon scattering. In that way the laser threshold is reduced and the laser output increased.²⁴⁻²⁸

Due to the efficiency of this coupling we suggest that, through the phonon sidebands reflecting the polaronic lattice distortion, elastic spin scattering becomes possible, leading to a destruction of the phase coherence. Dou-

ble phonon processes scattering out of one level and back into the same level may become efficient because the crystal offers a continuum of phonon states, enabling multiple scattering options. This scattering may explain the restriction of the hole spin coherence time to microseconds below 8 K and might also explain the speed-up of spin relaxation at higher temperatures. However, still more detailed studies need to be done.

In summary, we have studied the temperature dependence of the hole spin coherence time T_2 by making use of the spin mode-locking effect and all-optically created hole spin echoes. The sharp drop of T_2 from μs down

to ns below 20 K suggests that mechanisms considered so far based on the hyperfine coupling and the spin-orbit interaction are not adequate for explanation and that further considerations may be required. We suggested here an alternative mechanism relying on elastic scattering exploiting the broad phonon sidebands. Prospectives for the further coherent manipulation of hole spins include multi-echo techniques, which might be used in dynamic decoupling schemes by which the spin coherence time might be extended, like in NMR experiments.²⁹

This work was supported by the Deutsche Forschungsgemeinschaft and the BMBF project QuaHL-Rep.

-
- ¹ P. Fallahi, S. T. Yilmaz, and A. Imamoglu, *Phys. Rev. Lett.* **105**, 257402 (2010).
 - ² E. A. Chekhovich, A. B. Krysa, M. S. Skolnick, and A. I. Tartakovskii, *Phys. Rev. Lett.* **106**, 027402 (2011).
 - ³ S. Varwig, A. Schwan, D. Barmascheid, C. Müller, A. Greilich, I. A. Yugova, D. R. Yakovlev, D. Reuter, A. D. Wieck, and M. Bayer, *Phys. Rev. B* **86**, 075321 (2012).
 - ⁴ I. A. Merkulov, A. L. Efros, and M. Rosen, *Phys. Rev. B* **65**, 205309 (2002).
 - ⁵ A. V. Khaetskii, D. Loss, and L. Glazman, *Phys. Rev. Lett.* **88**, 186802 (2002).
 - ⁶ J. R. Petta, A. C. Johnson, J. M. Taylor, E. A. Laird, A. Yacoby, M. D. Lukin, C. M. Marcus, M. P. Hanson, and A. C. Gossard, *Science* **309**, 2180 (2005).
 - ⁷ A. Greilich, D. R. Yakovlev, A. Shabaev, A. L. Efros, I. A. Yugova, R. Oulton, V. Stavarache, D. Reuter, A. D. Wieck, and M. Bayer, *Science* **313**, 341 (2006).
 - ⁸ J. Fischer, and D. Loss, *Phys. Rev. Lett.* **105**, 266603 (2010).
 - ⁹ K. D. Greve, P. L. McMahon, D. Press, T. D. Ladd, D. Bisping, C. Schneider, M. Kamp, L. Worschech, S. Höfling, A. Forchel, and Y. Yamamoto, *Nature Physics* **7**, 872 (2011).
 - ¹⁰ F. Fras, B. Eble, B. Siarry, F. Bernardot, A. Miard, A. Lemaître, C. Testelin, and M. Chamorro, *Phys. Rev. B* **86**, 161303(R) (2012).
 - ¹¹ I. A. Yugova, A. Greilich, E. A. Zhukov, D. R. Yakovlev, M. Bayer, D. Reuter, and A. D. Wieck, *Phys. Rev. B* **75**, 195325 (2007).
 - ¹² A. Greilich, A. Shabaev, D. R. Yakovlev, A. L. Efros, I. A. Yugova, D. Reuter, A. D. Wieck, and M. Bayer, *Science* **317**, 1896 (2007).
 - ¹³ A. Greilich, Sophia E. Economou, S. Spatzek, D. R. Yakovlev, D. Reuter, A. D. Wieck, T. L. Reinecke, and M. Bayer, *Nature Physics* **5**, 262 (2009).
 - ¹⁴ F. G. G. Hernandez, A. Greilich, F. Brito, M. Wiemann, D. R. Yakovlev, D. Reuter, A. D. Wieck, and M. Bayer, *Phys. Rev. B* **78**, 041303(R) (2008).
 - ¹⁵ J. Fischer, W. A. Coish, D. V. Bulaev, and D. Loss, *Phys. Rev. B* **78**, 155329 (2008).
 - ¹⁶ C. Testelin, F. Bernardot, B. Eble, and M. Chamorro, *Phys. Rev. B* **79**, 195440 (2009).
 - ¹⁷ B. Eble, C. Testelin, P. Desfonds, F. Bernardot, A. Balocchi, T. Amand, A. Miard, A. Lemaître, X. Marie, and M. Chamorro, *Phys. Rev. Lett.* **102**, 146601 (2009).
 - ¹⁸ X. J. Wang, S. Chesi, and W. A. Coish, *Phys. Rev. Lett.* **109**, 237601 (2012).
 - ¹⁹ Y. G. Semenov and K. W. Kim, *Phys. Rev. B* **75**, 195342 (2007).
 - ²⁰ E. Zibik, A. Andreev, L. Wilson, M. Steer, R. Green, W. Ng, J. Cockburn, M. Skolnick, and M. Hopkinson, *Physica E (Amsterdam)* **26**, 105 (2005).
 - ²¹ H. Kurtze, J. Seebeck, P. Gartner, D. R. Yakovlev, D. Reuter, A. D. Wieck, M. Bayer, and F. Jahnke, *Phys. Rev. B* **80**, 235319 (2009).
 - ²² P. Borri, W. Langbein, S. Schneider, U. Woggon, R. L. Sellin, D. Ouyang, and D. Bimberg, *Phys. Rev. Lett.* **87**, 157401 (2001).
 - ²³ A. Vagov, V. M. Axt, and T. Kuhn, *Phys. Rev. B* **66**, 165312 (2002).
 - ²⁴ M. Kaniber, A. Laucht, A. Neumann, J. M. Villas-Boas, M. Bichler, M.-C. Amann, and J. J. Finley, *Phys. Rev. B* **77**, 161303(R) (2008).
 - ²⁵ D. Press, S. Götzinger, S. Reitzenstein, C. Hofmann, A. Löffler, M. Kamp, A. Forchel, and Y. Yamamoto, *Phys. Rev. Lett.* **98**, 117402 (2007).
 - ²⁶ K. Hennessy, A. Badolato, M. Winger, D. Gerace, M. Atatüre, S. Gulde, S. Fält, E. L. Hu, and A. Imamoglu, *Nature* **445**, 896 (2007).
 - ²⁷ M. Winger, T. Volz, G. Tarel, S. Portolan, A. Badolato, K. J. Hennessy, E. L. Hu, A. Beveratos, J. J. Finley, V. Savona, and A. Imamoglu, *Phys. Rev. Lett.* **103**, 207403 (2009).
 - ²⁸ S. Ates, S. M. Ulrich, A. Ulhaq, S. Reitzenstein, A. Löffler, S. Höfling, A. Forchel, and P. Michler, *Nature Photon.* **3**, 724 (2009).
 - ²⁹ H. Bluhm, S. Foletti, I. Neder, M. Rudner, D. Mahalu, V. Umansky, and A. Yacoby, *Nature Physics* **7**, 109 (2011).